OH radical reactions with phenylalanine in free and peptide forms†

Annia Galano*[a] and Armando Cruz-Torres[b]

Received 18th October 2007, Accepted 14th December 2007
First published as an Advance Article on the web 11th January 2008
DOI: 10.1039/b716024k

Density functional theory has been used to model the reaction of OH with L-phenylalanine, as a free molecule and in the Gly-Phe-Gly peptide. The influence of the environment has been investigated using water and benzene as models for polar and non-polar surroundings, in addition to gas phase calculations. Different paths of reaction have been considered, involving H abstractions and addition reactions, with global contributions to the overall reaction around 10% and 90% respectively when Phe is in its free form. The *ortho*-adducts (*o*-tyrosine) were found to be the major products of the Phe + OH reaction, for all the modeled environments and especially in water solutions. The reactivity of phenylalanine towards OH radical attacks is predicted to be higher in its peptidic form, compared to the free molecule. The peptidic environment also changes the sites' reactivity, and for the Gly-Phe-Gly + OH reaction H abstraction becomes the major path of reaction. The good agreement found between the calculated and the available experimental data supports the methodology used in this work, as well as the data reported here for the first time.

Introduction

The reactions of biological molecules with free radicals, especially when the latter are reactive oxygen species (ROS), are assumed to cause several diseases like cancer,[1] cardiovascular disorders,[2] and atherosclerosis.[3] In addition, most of the amino acids and their derivative synthesis have been based on ionic procedures in the past, but recently the realization that radical reactions can be performed with a high degree of regio- and stereocontrol[4–6] has contributed to the increased interest in this kind of reaction. The ROS ($^1O_2$, O_2^{-}, $H_2O_2^{\bullet}$, and $^{\bullet}OH$) are formed in vast quantities in each cell, as a result of normal oxygen metabolism. The most reactive ROS is the OH radical, and it can be formed intracellularly by a Fenton-type reaction, by Haber–Weiss recombination, *via* water radiolysis, or by other radicals created from enzyme reactions.[7–11] OH radicals can also be produced by ultraviolet and ionizing radiation.[12] Due to its abundance and high reactivity the hydroxyl radical ($^{\bullet}OH$) was chosen for this study. The exposure of proteins to hydroxyl radicals, or to the combination of them with the superoxide anion radical, causes gross structural modifications. Such modified proteins can undergo spontaneous fragmentation or can exhibit a substantial increase in their proteolytic susceptibility.[13]

Phenylalanine (F, Phe, $C_9H_{11}NO_2$) is an essential α-amino acid. As its name suggests it is a derivative of alanine with a phenyl substituent on the β carbon, and has been classified as nonpolar because of the hydrophobic nature of the benzyl side chain. Phenylalanine plays a key role in the biosynthesis of other amino acids and some neurotransmitters. It is the most commonly found aromatic amino acid in proteins and enzymes with a molar ratio of 3.5 percent compared to the other amino acids, about double the amount of any other aromatic amino acid. Accordingly, its susceptibility to damage by ROS species is of great interest. It has been proposed that Phe20 in β-amyloid (βA) plays a role in the oxidative damage associated with Alzheimer's disease through long distance electron transfer (ET).[14] Even though the ET mechanism was recently refused, it has been proven that when Phe20 is replaced by alanine, oxidation and mitochondrial functions are affected to a lesser extent.[15] This finding might be explained by direct reactions of ROS with Phe in βA. As a free molecule, Phe enters human bodies through the intake of the widely used artificial sweetener aspartame, which releases Phe when hydrolyzed.[16] This process leads to a sharp increase in plasma phenylalanine, which is assumed to be converted into *para*-tyrosine by phenylalanine hydroxylase. However its reaction with OH radicals can also lead to the non-natural isomers *ortho*- and *meta*-tyrosine, which are considered biomarkers of oxidative damage as free or protein-bounded amino acids.[17]

As well as other biological molecules,[18,19] Phe is vulnerable to oxidative damage. Since the site of the initial attack can determine the outcoming products, it is relevant to know what are the most reactive sites and in what proportion the initial oxidation products are expected to be formed. It has been reported that α-carbon-centered radicals are most likely to occur for the aliphatic amino acids and their derivatives.[20] For aromatic amino acids, on the other hand, adduct formation is expected to contribute to the overall reaction to a significant extent.[21–27] However, to our best knowledge, there are no previous studies providing detailed comparisons of the contributions of the different pathways to the overall Phe + OH reaction. There is also a lack of knowledge about the transition structures and the mechanism, and about the influence of the polarity of the environment on the rate coefficients.

[a]*Departamento de Química, Universidad Autónoma Metropolitana-Iztapalapa, San Rafael Atlixco 186, Col. Vicentina. Iztapalapa. C. P., 09340, México, D. F., México. E-mail: agalano@prodigy.net.mx*
[b]*Instituto Mexicano del Petróleo, Eje Central Lázaro Cárdenas 152, 007730, México, D. F., México*

† Electronic supplementary information (ESI) available: Cartesian coordinates of optimized transition states of Phe + OH and GFG + OH reactions; entropies of reaction and entropy barriers for Phe + OH and GFG + OH reactions in gas phase and solution; intrinsic reaction coordinate calculations for R*a* and R*oa* reaction paths; colour versions of article figures. See DOI: 10.1039/b716024k

Therefore, the objective of this work is to provide quantitative information about the mechanism and kinetics of this reaction, which can be considered as the very first step in the oxidative damage of Phe. It is also our purpose to propose branching ratios for the different channels of reaction. In addition the OH reaction with phenylalanine in the peptide Gly-Phe-Gly has also been studied to mimic the peptidic environment, as well as the influence of the solvent polarity using water and benzene as models for polar and non-polar surroundings.

Computational details

Electronic structure calculations have been performed with the Gaussian 03[28] program. Full geometry optimizations and frequency calculations were carried out for all the stationary points using the B3LYP hybrid HF-density functional and the 6-311G(d,p) basis set. The energies of all the stationary points were improved by single point calculations at the B3LYP/Aug-cc-pvTZ level of theory. This functional has been chosen based on its previously described success to study systems of similar size and structures to those modeled in the present work.[29] Thermodynamic corrections at 298 K were included in the calculation of relative energies. Restricted calculations were used for closed shell systems and unrestricted ones for open shell systems. Local minima and transition states were identified by the number of imaginary frequencies (NIMAG = 0 or 1, respectively). In addition, the vibrational modes with imaginary frequencies were inspected using the GaussView[30] program, and it was confirmed that they do connect the corresponding reactants and products. For selected paths of reaction, involving free Phe, Intrinsic Reaction Coordinate (IRC) calculations were carried out at the B3LYP/6-311G(d,p) level of theory and it was corroborated that the transition states properly connect reactants and products. Two of these IRCs, one for an addition channel and another one for an abstraction channel, have been provided as supplementary information (Figures S1 and S2†).

The stationary points were first modeled in gas phase (vacuum), and solvent effects were included *a posteriori* by single point calculations using the polarizable continuum model, specifically the integral-equation-formalism (IEF-PCM)[31] at the B3LYP/Aug-cc-pvTZ level of theory, with water and benzene as solvents for polar and non-polar environments, respectively. In PCM calculations, the choice of the solute cavity is important because the computed energies and properties strongly depend on the cavity size. For the addition reaction channels the cavity was computed using the simple united atom topological model (UA0), which is the default option in Gaussian 03. In this model hydrogen atoms have no individual sphere but are included in the same sphere of the heavy atom they are bonded to, which rules out its use for H abstraction reactions. Therefore, for the abstraction channels atomic radii from the universal force field were used (RADII = UFF), in which case hydrogens are assigned individual spheres (explicit hydrogens). Radii for extra spheres added to smooth the cavity were set to have a minimum value of 0.5 Å (RMIN = 0.5), and the overlap index between interlocking spheres was set to 0.8 (OFAC = 0.8). A similar approach, using different solute cavities for addition and abstraction reactions involving OH radicals, has been previously used with success.[32]

The rate constants (k) were calculated using Conventional Transition State Theory (TST)[33–35] and 1 M standard state as:

$$k = \sigma \frac{k_B T}{h} e^{-\Delta G^{\neq}/RT} \quad (1)$$

where k_B and h are the Boltzman and Planck constants, $\Delta G^{\neq}$ is the Gibbs free energy of activation, and σ represents the reaction path degeneracy, accounting for the number of equivalent reaction paths. Tunneling factors are not included since they were found to be negligible in all cases.

Results and discussion

The different reactive sites that have been studied in the present work are schematically represented in Fig. 1. The letters *a*, *b*, *i*, *o*, *m*, and *p* stand for •OH attacks on alpha, beta, *ipso*, *ortho*, *meta* and *para* sites, respectively. The two first correspond to H abstraction reactions and all the rest to •OH additions to the ring. For the addition channels, and due to the internal rotation around the C_i–C_β axis, the sites *o* and *o*′ (*m* and *m*′) are equivalent and there are four different sites for the addition to take place. However, if we take the phenyl ring as a reference plane, the transition states (TS) involved in the OH radical attack to any of these sites can show *syn* or *anti* structures with respect to the amino acid end. Since the energies of these two forms can significantly differ, eight transition structures have been considered in this work, and the reaction paths have been named accordingly (Fig. 1). It also should be noted that for *ortho* and *meta* additions, the *anti* and *syn* transition states lead to different products since a new chiral center is formed. Accordingly, and since phenylalanine has been modeled in its *S* form which correspond to the biologically-active enantiomer (L species), the *syn–ortho* TS leads to an *RS* product, while an *SS* adduct is formed through the *anti–ortho* TS. In the same way paths R*ms* and R*ma* are involved the formation of *SS* and *RS meta* adducts, respectively.

The optimized geometries of the transition states (TS) involved in all the modeled reaction paths are shown in Fig. 2 (and Cartesian coordinates are reported as supplementary information in Table S1†). As this figure shows, for the addition channels the *anti*-TSs were found to be earlier than the *syn*-TSs. Among the *anti*-TSs, leading to *ortho* •OH addition was found to be the earliest one, while among the *syn*-TSs the earliest one is that corresponding to the *ipso* addition. However, all the O···C distances are very similar, around 2.0 Å, suggesting that all the addition channels should have similar heats of reaction. For H abstraction channels, the alpha TS was found to be significantly earlier than the beta TS, with the O···H (C···H) distance larger (shorter) by 0.23 Å (0.07 Å), suggesting that alpha abstraction products should be lower in energy compared to beta abstraction products.

The values of the Gibbs free energies of reaction (ΔG_{gas}) and barriers ($\Delta G_{gas}^{\neq}$) at 298.15 K for the different reaction paths involved in the Phe + OH gas phase reaction are reported in Table 1. As the values in this table show, all the channels are predicted to be exergonic. In addition, the energy releases associated with the adduct formation are smaller, with Gibbs free energies of reaction more than 20 kcal mol^{-1} higher, than those of the abstraction paths. The largest exergonicity was found for the alpha abstraction. The reaction barriers range from 7.5 to 13.8 kcal mol^{-1}. As the geometries of the transition states suggested

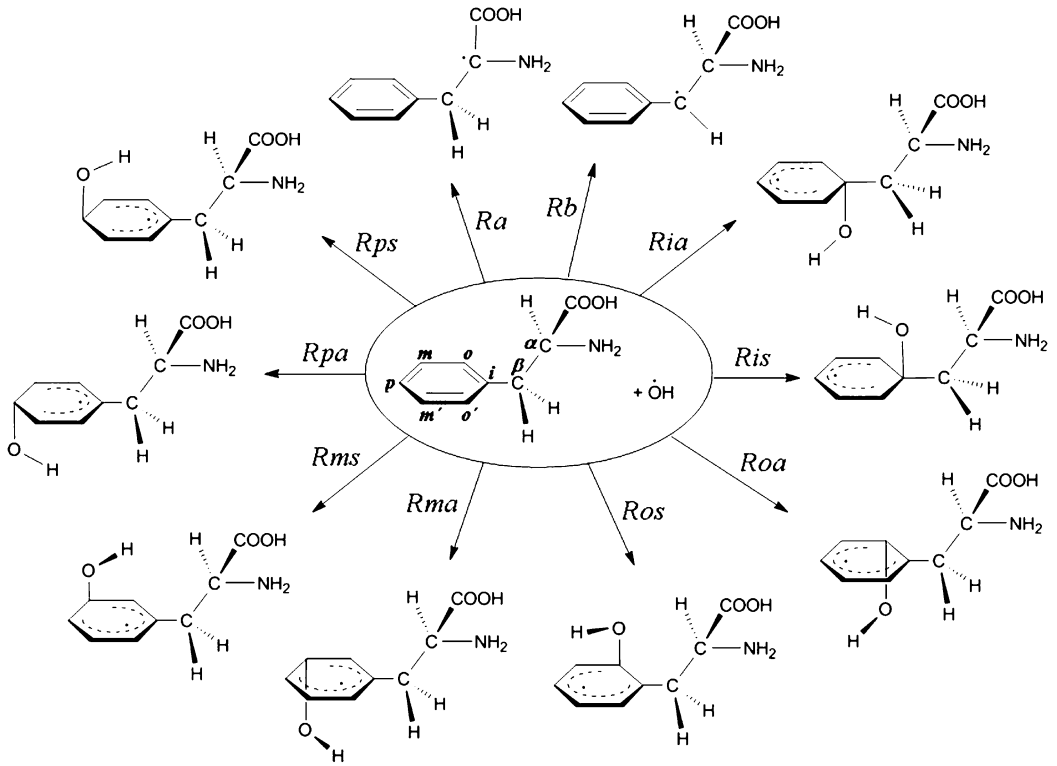

Fig. 1 Schematic representation of the studied paths of reaction, based on the transition state structures.

Table 1 Gibbs free energies of reaction (ΔG_{gas}) and barriers ($\Delta G_{gas}^{\neq}$) at 298.15 K, all in kcal mol^{-1}, for the modeled channels of the Phe + OH gas phase reaction

	$\Delta G_{gas}^{\neq}$	ΔG_{gas}
R*a*	7.90	−44.67
R*b*	9.92	−29.80
R*ia*	9.81	−1.63
R*is*	13.84	−1.63
R*oa*	7.67	−3.96
R*os*	10.29	−3.04
R*ma*	8.48	−2.80
R*ms*	8.50	−2.71
R*pa*	8.41	−3.59
R*ps*	7.50	−3.59

the barrier for channel R*a* is lower than that of channel R*b*, by about 2 kcal mol^{-1}, indicating that OH hydrogen abstractions mainly occur from alpha sites, in the gas phase. For the *ortho* addition the barrier corresponding to the *anti*-TS is lower than that of *syn* channel by 2.6 kcal mol^{-1}, suggesting that *ortho* adducts should be formed almost exclusively as *SS* isomers. For the *meta* additions, on the other hand, the *syn* and *anti* barriers are of similar magnitude and the *RS* and *SS* adducts are expected to occur in similar proportions.

Up to this point, all the reported energies correspond to the gas phase, using a standard state of 1 atm, as calculated from the Gaussian program outputs. However, for reactions in solution the reference state has been changed from 1 atm to 1 M and the solvent cage effects have been included according to the corrections proposed by Okuno,[36] taking into account the free volume theory.[37] These corrections are in good agreement with those independently obtained by Ardura *et al.*[38] and have been successfully used by other authors.[39,40] The expression used to correct the Gibbs free energy is:

$$\Delta G^{sol} \cong \Delta G^{gas} - RT\{\ln[n10^{(2n-2)}] - (n-1)\} \quad (2)$$

where n represents the total of reactant moles. According to eqn (2), the cage effects in solution cause ΔG^{sol} to decrease by 2.54 kcal mol^{-1} for bimolecular reactions, at 298 K, with respect to ΔG^{gas}. This lowering is expected since the cage effects of the solvent reduce the entropy loss associated with any addition reaction or transition state formation, in reactions with molecularity equal to or larger than two. Therefore, if the translational degrees of freedom in solution are treated as in the gas phase, the cost associated with their loss when two or more molecules form a complex system in solution is overestimated, and consequently these processes are kinetically over-penalized in solution leading to rate constants that are artificially underestimated.

The Gibbs free energies of reaction (ΔG_{sol}) and barriers ($\Delta G_{sol}^{\neq}$) at 298.15 K, for the modeled channels of the Phe + OH reaction in solution, with water and benzene as solvents, are shown in Table 2. Comparing the values in this table with those in Table 1, it is evident that the presence of a solvent increases the exergonicity of all the reaction paths. The reaction barriers were found to be systematically higher in the gas phase than in solution and the lowest barriers for all the studied paths were those modeled with benzene as solvent. For the abstraction channels the presence of the polar solvent inverts the site reactivity, *i.e.* the barriers for abstractions from the *beta* site become lower than those for *alpha* abstractions. For the addition channels, on the other hand, the relative barrier heights involving *anti* and *syn* TSs in solution retain the same order as in gas phase. However, for *meta* adducts the difference between $\Delta G_{sol}^{\neq}$(R*ma*) and $\Delta G_{sol}^{\neq}$(R*ms*) is significantly

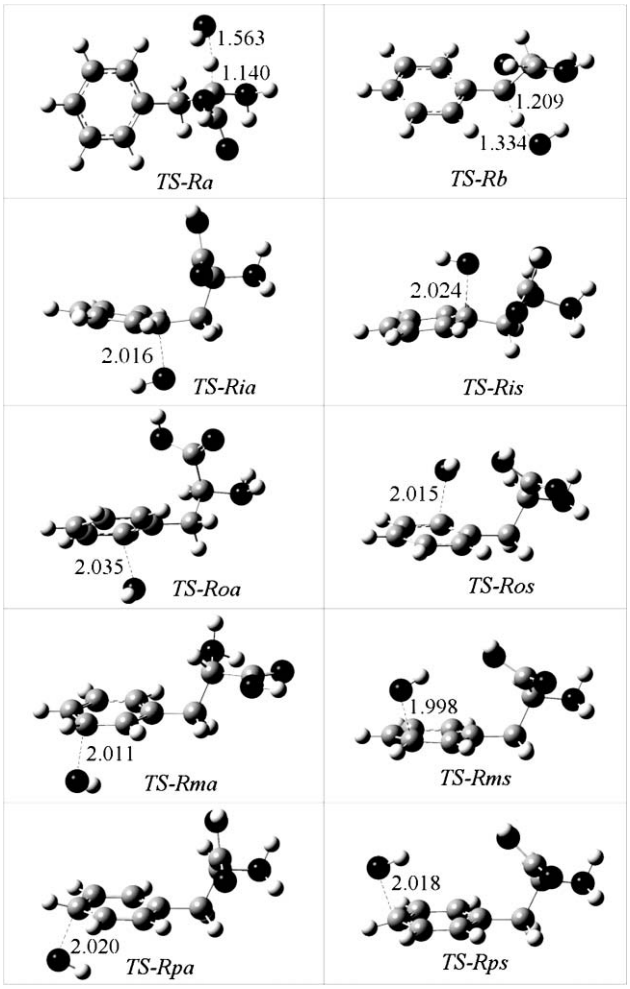

Fig. 2 Fully optimized geometries of the Phe + OH transition states.

Table 2 Gibbs free energies of reaction (ΔG_{sol}) and barriers ($\Delta G_{sol}^{\neq}$) at 298.15 K, all in kcal mol^{-1}, for the modeled channels of Phe + OH reaction in water and benzene solutions

	Water		Benzene	
	$\Delta G_{sol}^{\neq}$	ΔG_{sol}	$\Delta G_{sol}^{\neq}$	ΔG_{sol}
R*a*	6.95	−44.72	5.25	−45.03
R*b*	5.72	−30.80	5.65	−30.18
R*ia*	7.73	−2.96	6.71	−4.23
R*is*	12.23	−2.96	10.27	−4.23
R*oa*	4.73	−5.11	4.23	−6.71
R*os*	9.19	−1.83	6.78	−5.28
R*ma*	6.07	−4.38	5.21	−6.26
R*ms*	7.12	−4.06	5.59	−5.89
R*pa*	5.36	−5.87	4.94	−7.22
R*ps*	5.28	−5.87	4.21	−7.22

larger in solution than in gas phase, especially in water, which suggests that in this solvent a larger proportion of the RS adduct should be present.

In order to illustrate the relevance of the entropy for the studied paths, values of the $-T\Delta S$ term have also been included as supplementary information (Tabla S2)† for reactions in solution and in the gas phase. As these values show, the entropy changes involved in the studied addition products and in all transition states are relatively large and they must be taken into account. In addition it seems relevant to notice that entropy loss in the gas phase is larger than in solution, as expected.

Table 3 Overall rate constants (L mol^{-1} s^{-1}) at 298.15 K, and branching ratios (Γ) for the modeled channels of the Phe + OH reaction

	Gas	Water	Benzene
k_{298}	1.96×10^9	7.14×10^9	2.13×10^{10}
Γ_{Ra}	0.125	0.007	0.041
Γ_{Rb}	0.008	0.111	0.042
Γ_{Ria}	0.005	0.002	0.004
Γ_{Ris}	0.000	0.000	0.000
Γ_{Roa}	0.372	0.589	0.464
Γ_{Ros}	0.004	0.000	0.006
Γ_{Rma}	0.094	0.062	0.089
Γ_{Rms}	0.091	0.010	0.047
Γ_{Rpa}	0.053	0.102	0.070
Γ_{Rps}	0.248	0.117	0.238

The branching ratios (Γ) of the different modeled paths of reaction are reported in Table 3, together with the values of the overall rate constants at 298 K. The branching ratios were calculated as:

$$\Gamma_{path} = \frac{k_{path}}{k_{overall}} \quad (3)$$

in such way that the rate constant for each path can be easily obtained from the values in Table 3 by multiplying the overall rate constant by the corresponding Γ value. The rate constant for the Phe + OH reaction in aqueous solution has been previously reported by different authors,[41–44] with an average value of 6.7×10^9 L mol^{-1} s^{-1} and the individual values ranging from 6.5 to 6.9×10^9 L mol^{-1} s^{-1}. The agreement of the rate constant calculated in this work with these previous reports is excellent, with only about 7% error. In addition, Solar[43] estimated that, in water solution, 50%, 14% and 30% of the reaction products correspond to *ortho*, *meta* and *para* adducts (tyrosines), respectively. The calculated values are 59%, 7% and 22%, which are also in line with the experimental data. The agreement between the calculated and the available experimental data supports the methodology used in this work, as well as the data reported here for the first time.

The percentage contributions of the different channels ($100 \times \Gamma$) to the overall rate constant have been plotted in Fig. 3 to help visualizing the abundant data obtained. Analyzing the results reported in Table 3 or Fig. 2, it can be easily seen that regardless of the polarity of the environment the formation of *ipso*-adducts can be neglected since the corresponding paths of reaction contribute to the overall rate constant by less than 1% in all the cases. This result is in line with previous calculations on toluene + OH reaction. For this system 3% *ipso* addition has been reported,[29b] which is very similar to our result for Phe. For xylenes + OH reactions, on the other hand, the calculated barriers associated with *ipso* additions are similar in height to those involving additions to other sites of the ring.[45] However, for *p*-xylene branching ratios of 80% and 20% have been recently proposed for *ortho* and *ipso* additions, respectively.[46] The main products of the OH + Phe reaction are the *ortho*-adducts (*o*-tyrosine) in all the modeled media, and as the polarity of the environment increases, so does the extent to which the *ortho*-adduct are formed: 38%, 47% and 59% in gas phase, benzene and water solution, respectively. In addition the *ortho*-adducts

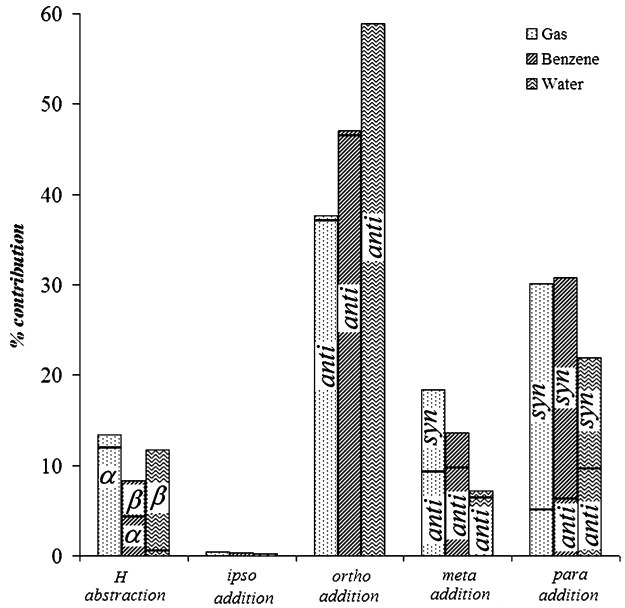

Fig. 3 Percentage contribution of the different channels to the Phe + OH overall reaction.

are expected to be formed almost exclusively as *SS* enantiomers since more than 98% of these products are predicted to be formed through the *anti*-TS structure. On the other hand the extent to which *meta* adducts are formed decreases from gas phase (18%) to benzene (13%) to water solution (7%). The environment also seems to influence the proportion of *RS* and *SS meta* adducts; while in the gas phase both are predicted to be formed to similar extent, in water the *RS* enantiomer is expected to be much more likely to occur. The finding that the extent of OH adduct formation in the Phe reaction follows the order *ortho* > *para* > *meta* > *ipso* is in line with what has been reported for toluene + OH reactions.[29b]

The contribution of H abstractions to the overall reaction does not significantly vary with the environment, ranging from 8% to 13%. On the other hand the site reactivity of H abstraction channels seems to be very sensitive to the environment. In the gas phase about 94% of the total H abstractions are predicted to occur from alpha sites, in benzene solution alpha and beta abstractions are predicted to be equally likely to occur, and in water solution only 6% of the H abstractions are predicted to involve alpha H.

In addition to the •OH reaction with phenylalanine as a free molecule, the OH reaction with the peptide glycine-phenylalanine-glycine (GFG) has also been modeled to mimic the influence of the peptidic environment on the reactivity of phenylalanine towards the OH radical. The peptide has been modeled in β-sheet conformation, since it corresponds to the structure of β-amyloid, obviously in solution.[47] It should be noticed that the same structure has been used in gas phase and solvent-based calculations, since geometry optimizations were performed only in the gas phase. This also means that the β-sheet structure is, at least, a local minimum in the gas phase. According to the fully optimized geometry of the peptide, the accessibility to one of the ring faces is highly hindered by the backbone. Therefore, additions through *anti*-TSs are the only ones that have been considered and based on the results discussed above for free Phe the formation of *ipso*-adducts has been ignored. The structures of the transition states are shown in Fig. 4, where the most relevant geometrical parameters have been explicitly included. The Cartesian coordinates are reported as supplementary information in Table S3.†

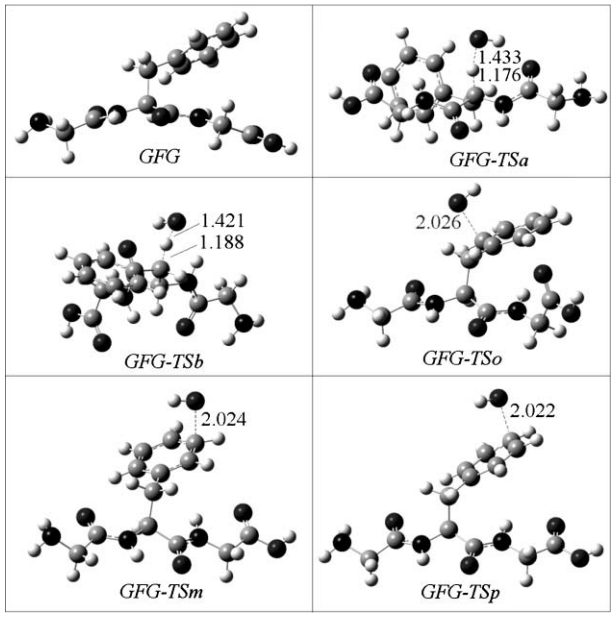

Fig. 4 Fully optimized geometries of GFG + OH transition states.

The Gibbs free energies of reaction (ΔG_{sol}) and barriers ($\Delta G_{sol}^{\neq}$) at 298.15 K, for the modeled channels of the GFG + •OH reaction in gas phase and in solution, with water and benzene as solvents, are shown in Table 4. All the reaction channels were found to be exergonic with ΔG values similar to those involving free phenylalanine. On the other hand the reaction barriers of •OH + GFG are smaller than those of •OH + Phe for abstraction channels and *para* additions, while for the *ortho* additions they increase by more than 3 kcal mol^{-1}. Changes in entropy have also been reported as supplementary information (Table S4)†, and similar trends to those previously discussed for the free form of Phe are found.

The overall rate constants at 298 K and the branching ratios (Γ) of the different modeled paths of the GFG + OH reaction are reported in Table 5. Comparing the values in this table with those in Table 3, it can be easily seen that the presence of the peptidic environment significantly increases the overall rate constants. The reaction of Phe with OH becomes about 2 and 9 times faster in water and benzene, respectively, with this amino acid in a peptidic environment. In addition, and analogously to what was found for free phenylalanine, the presence of solvents also causes an

Table 4 Gibbs free energies of reaction (ΔG) and barriers ($\Delta G^{\neq}$) in kcal mol^{-1}, for the modeled channels of the GFG + OH reaction in gas phase and in water and benzene solutions

	Gas phase		Water		Benzene	
	$\Delta G^{\neq}$	ΔG	$\Delta G^{\neq}$	ΔG	$\Delta G^{\neq}$	ΔG
Alpha	5.20	−34.92	4.18	−35.71	2.32	−21.82
Beta	6.29	−29.42	4.50	−32.02	3.24	−30.30
ortho	10.74	−1.09	8.62	−2.76	7.45	−3.81
meta	9.36	−3.10	6.99	−3.85	5.73	−6.14
para	8.06	−3.66	4.40	−5.40	3.41	−7.12

Table 5 Overall rate constants (L mol^{-1} s^{-1}) at 298.15 K, and branching ratios (Γ) for the modeled channels of the GFG + OH reaction in gas phase, and in water and benzene solutions

	Gas phase	Water	Benzene
k_{298}	3.09×10^{10}	1.54×10^{10}	1.96×10^{11}
Γ_{Ra}	0.752	0.347	0.627
Γ_{Rb}	0.240	0.405	0.268
Γ_{Ro}	0.000	0.000	0.000
Γ_{Rm}	0.001	0.006	0.004
Γ_{Rp}	0.006	0.242	0.101

increment of the GFG + OH rate constant and the fastest process occurs in benzene, *i.e.* in non-polar solution. It could be important to notice that the values in Table 5 represent upper limits of k_{298}, since TST is expected to overestimate these values. Due to the size of the studied system, variational TST would be extremely expensive and we have decided to use conventional TST instead, since this approach is expected to reproduce correctly the trends on sites' reactivity.

The increase in the overall rate coefficient caused by the peptidic environment is essentially caused by the significant increment of the alpha site reactivity. Analyzing the structure of the corresponding transition states it can be seen that in both cases there is a stabilizing intra-molecular hydrogen bond interaction, between the H atom in the OH radical and one of the oxygen atoms in the other reactant. For free Phe this interaction involves the hydroxylic oxygen in the carboxylic group, while in the GFG peptide it involves a carbonyl oxygen from the backbone. The H $\cdots$ O distances for these H bonds are 1.99 and 2.31 Å for GFG and Phe, respectively, indicating that there is a stronger interaction in the peptide, leading to a lower barrier. To find an explanation for this higher strength the atomic charges on both O atoms were analyzed in the reactants, and it was found that the charge on the O in the peptide is significantly more negative (−0.92) than in the free molecule (−0.48), which explains the stronger interaction with the H atom in the OH radical (+0.24). While these intra-molecular H bond interactions are viable in the TSs of the Phe + OH reaction for both abstraction and addition channels, they only seem to be viable in GFG for the abstraction channels. This implies lower barriers for the abstraction paths (in GFG) and might explain why they become the main channels in the peptide.

The presence of the peptidic environment does not only increase the overall reactivity of phenylalanine toward OH radicals, but also changes the relative reactivity of the different sites of reaction. When phenylalanine is modeled in the GFG tri-peptide the contributions of *ortho* additions to the overall reaction become negligible. The percentage contribution of H abstractions to the overall reaction is predicted to be around 88% and 74% in benzene and water solutions, respectively, when phenylalanine is in the GFG peptide. In addition alpha abstractions are the processes most likely to occur, in non-polar environments, while in water beta H abstraction is predicted to be slightly favored. Since the difference in reactivity for H abstractions from alpha and beta sites was found to be rather small in water it is expected that both kinds of products are formed to significant extent. Among the addition reactions, only those leading to *para*-adduct formation are predicted to significantly contribute to the overall reaction. In general the obtained data for GFG suggest that the higher the polarity of the solvent the wider the product distribution.

Conclusions

Different paths of reaction have been considered, involving H abstractions from and OH additions to phenylalanine in its free form and as part of the GFG peptide. The global contributions of H abstractions to the overall reaction were found to be around 10% and 80% when F is in its free form and in GFG, respectively. The *ortho*-adducts (*o*-tyrosine) were found to be the major products of the F + OH reaction, for all the modeled environments and especially in water solutions. The reactivity of phenylalanine towards OH radical attacks is predicted to be higher in its peptidic form, compared to the free molecule. The presence of the peptidic environment was found to strongly influence the relative site reactivity of phenylalanine, and H abstraction reactions are predicted to be the main channels of reaction for F in the GFG peptide. The good agreement found between the calculated and the available experimental data supports the methodology used in this work, as well as the data reported here for the first time.

Acknowledgements

The authors thank Prof. M. A. Iglesias-Arteaga for his valuable comments. A.G. also thanks the SEPCONACYT grant SEP-2004-C01-46167 for the financial support.

References

1 (*a*) N. F. Boyd and V. McGuire, *Free Radical Biol. Med.*, 1991, **10**, 185; (*b*) R. L. Nelson, *Free Radical Biol. Med.*, 1992, **12**, 161; (*c*) P. Knekt, A. Reunanen, H. Takkunen, A. Aromaa, M. Heliovarara and T. Hakulinen, *Int. J. Cancer*, 1994, **56**, 379; (*d*) G. S. Omenn, G. E. Goodman and M. D. Thornquist, *N. Engl. J. Med.*, 1996, **334**, 1150.
2 (*a*) R. A. Riemmersma, D. A. Wood, C. C. A. Macityre, R. A. Elton, K. F. Gey and M. F. Oliver, *Lancet*, 1991, **337**, 1; (*b*) J. T. Salonen, K. Nyyssoner, H. Korpela, J. Tuomilehto, R. Seppanen and R. Salonen, *Circulation*, 1992, **86**, 803; (*c*) D. A. Street, G. Comstock, R. Salkeldy and M. Klag, *Circulation*, 1994, **90**, 1154; (*d*) L. H. Kushi, A. R. Folsom, R. J. Prineas, P. J. Mink, Y. Wu and R. Bostick, *N. Engl. J. Med.*, 1996, **334**, 1156; (*e*) N. G. Stephens, A. Parsons, P. M. Schofield, F. Kelly, K. Cheesman, M. J. Mitchisnon and M. J. Brown, *Lancet*, 1996, **347**, 781.
3 (*a*) O. M. Panasenko, T. V. Nova, O. A. Azizova and Y. A. Vladimirov, *Free Radical Biol. Med.*, 1991, **10**, 137; (*b*) D. Steinberg, *Circulation*, 1991, **84**, 1421; (*c*) D. R. Janero, *Free Radical Biol. Med.*, 1991, **11**, 129; (*d*) H. N. Hodis, W. J. Mack, L. LaBree, L. Cashin-Hemphill, A. Sevanian, R. Johnson and S. Azen, *J. Am. Med. Assoc.*, 1995, **273**, 1849.
4 A. L. J. Beckwith, *Tetrahedron*, 1981, **37**, 3073.
5 B. Giese, *Radicals in Organic Synthesis*, Pergamon Press, Oxford, 1986.
6 D. P. Curran, *Synthesis*, 1988, 417.
7 H. Sies, *Oxygen Stress*, Academic Press, London, 1985.
8 M. G. Simic, K. A. Taylor, J. F. Ward, C. Von Sonntag, *Oxygen Radicals in Biology and Medicine*, Plenum Press, New York, 1991.
9 K. J. A. Davies, *Oxydative Damage and Repair: Chemical, Biological and Medical Aspects*, Pergamon Press, New York, 1991.
10 H. Sies, *Oxygen Stress-Oxidants and Anti-Oxidants*, Academic Press, London, 1991.
11 E. R. Stadtman, *Annu. Rev. Biochem.*, 1993, **62**, 797.
12 C. Von Sonntag, *The Chemical Basis of Radiation Biology*, Taylor & Francis, London, 1987.
13 K. J. Davies, M. E. Delsignore and S. W. Lin, *J. Biol. Chem.*, 1987, **262**, 9902.
14 D. Pogocki, *Chem. Res. Toxicol.*, 2004, **17**, 325.
15 D. Boyd-Kimball, H. M. Abdul, T. Reed, R. Sultana and D. A. Butterfield, *Chem. Res. Toxicol.*, 2004, **17**, 1743.
16 See for example: (*a*) N. A. Tobey and W. D. Heizer, *Gastroenterology*, 1986, **91**, 931; (*b*) S. L. Burgert, D. W. Andersen, L. D. Stegink, H. Takeuchi and H. P. Schedl, *Metabolism*, 1991, **40**, 612.
17 B. C. Blount and M. W. Duncan, *Anal. Biochem.*, 1997, **244**, 270.
18 M. M. Greenberg, *Org. Biomol. Chem.*, 2007, **5**, 18.

19 K. Ohkubo, Y. Moro-oka and S. Fukuzumi, *Org. Biomol. Chem.*, 2006, **4**, 999.
20 C. J. Easton, in *Advances in Detailed Reaction Mechanisms*, ed. J. M. Coxon, JAI Press, London, 1991, vol. 1.
21 S. Ishimitsu, S. Fujimoto and A. Ohara, *Chem. Pharm. Bull.*, 1990, **38**, 1417.
22 T. G. Huggins, M. C. Wells-Knecht, N. A. Detorie, J. W. Baynes and S. R. Thorpe, *J. Biol. Chem.*, 1993, **268**, 12341.
23 P. F. Fitzpatrick, *J. Am. Chem. Soc.*, 1994, **116**, 1133.
24 H. Kaur and B. Halliwell, *Methods Enzymol.*, 1994, **233**, 67.
25 P. J. Hillas and P. F. Fitzpatrick, *Biochemistry*, 1996, **35**, 6969.
26 C. Leeuwenburgh, P. Hansen, A. Shaish, J. O. Holloszy and J. W. Heinecke, *Am. J. Physiol.: Regul., Integr. Comp. Physiol.*, 1998, **274**, 453.
27 J. A. Pavon and P. F. Fitzpatrick, *Biochemistry*, 2006, **45**, 11030.
28 M. J. Frisch, G. W. Trucks, H. B. Schlegel, G. E. Scuseria, M. A. Robb, J. R. Cheeseman, J. A. Montgomery, Jr., T. Vreven, K. N. Kudin, J. C. Burant, J. M. Millam, S. S. Iyengar, J. Tomasi, V. Barone, B. Mennucci, M. Cossi, G. Scalmani, N. Rega, G. A. Petersson, H. Nakatsuji, M. Hada, M. Ehara, K. Toyota, R. Fukuda, J. Hasegawa, M. Ishida, T. Nakajima, Y. Honda, O. Kitao, H. Nakai, M. Klene, X. Li, J. E. Knox, H. P. Hratchian, J. B. Cross, V. Bakken, C. Adamo, J. Jaramillo, R. Gomperts, R. E. Stratmann, O. Yazyev, A. J. Austin, R. Cammi, C. Pomelli, J. Ochterski, P. Y. Ayala, K. Morokuma, G. A. Voth, P. Salvador, J. J. Dannenberg, V. G. Zakrzewski, S. Dapprich, A. D. Daniels, M. C. Strain, O. Farkas, D. K. Malick, A. D. Rabuck, K. Raghavachari, J. B. Foresman, J. V. Ortiz, Q. Cui, A. G. Baboul, S. Clifford, J. Cioslowski, B. B. Stefanov, G. Liu, A. Liashenko, P. Piskorz, I. Komaromi, R. L. Martin, D. J. Fox, T. Keith, M. A. Al-Laham, C. Y. Peng, A. Nanayakkara, M. Challacombe, P. M. W. Gill, B. G. Johnson, W. Chen, M. W. Wong, C. Gonzalez and J. A. Pople, *GAUSSIAN 03 (Revision D.01)*, Gaussian, Inc., Wallingford, CT, 2004.
29 See for example: (*a*) C. Barckholtz, T. A. Barckholtz and C. M. Hadad, *J. Phys. Chem. A*, 2001, **105**, 140; (*b*) I. Suh, D. Zhang, R. Zhang, L. T. Molina and M. J. Molina, *Chem. Phys. Lett.*, 2002, **364**, 454; (*c*) A. Bassan, M. R. A. Blomberg and P. E. M. Siegbahn, *Chem.–Eur. J.*, 2003, **9**, 4055; (*d*) J. Casanovas, A. I. Jimenez, C. Cativiela, J. J. Perez and C. Aleman, *J. Org. Chem.*, 2003, **68**, 7088; (*e*) G. L. Boroskya and A. B. Pierini, *Org. Biomol. Chem.*, 2005, **3**, 649; (*f*) H. Lioea and R. A. J. O'Hair, *Org. Biomol. Chem.*, 2005, **3**, 3618; (*g*) A. Kaczor, I. D. Reva, L. M. Proniewicz and R. Fausto, *J. Phys. Chem. A*, 2006, **110**, 2360; (*h*) P. Fiedler, S. Bohm, J. Kulhanekc and O. Exner, *Org. Biomol. Chem.*, 2006, **4**, 2003.
30 R. Dennington IIT. KeithJ. MillamK. EppinnettW. L. HovellR. Gilliland, *GaussView, Version 3.0*, Semichem, Inc., Shawnee Mission, KS, 2003.
31 (*a*) M. T. Cances, B. Mennucci and J. Tomasi, *J. Chem. Phys.*, 1997, **107**, 3032; (*b*) B. Mennucci and J. Tomasi, *J. Chem. Phys.*, 1997, **106**, 5151; (*c*) B. Mennucci, E. Cances and J. Tomasi, *J. Phys. Chem. B*, 1997, **101**, 10506; (*d*) J. Tomasi, B. Mennucci and E. Cances, *THEOCHEM*, 1999, **464**, 211.
32 A. S. Ozen, V. Aviyente, G. Tezcanli-Guyer and N. H. Ince, *J. Phys. Chem. A*, 2005, **109**, 3506.
33 H. Eyring, *J. Chem. Phys.*, 1935, **3**, 107.
34 M. G. Evans and M. Polanyi, *Trans. Faraday Soc.*, 1935, **31**, 875.
35 D. G. Truhlar, W. L. Hase and J. T. Hynes, *J. Phys. Chem.*, 1983, **87**, 2664.
36 Y. Okuno, *Chem.–Eur. J.*, 1997, **3**, 212.
37 S. W. Benson, *The Foundations of Chemical Kinetics*, Krieger, FL, 1982.
38 D. Ardura, R. Lopez and T. L. Sordo, *J. Phys. Chem. B*, 2005, **109**, 23618.
39 J. R. Alvarez-Idaboy, L. Reyes and J. Cruz, *Org. Lett.*, 2006, **8**, 1763.
40 A. Galano, *J. Phys. Chem. A*, 2007, **111**, 1677, (*Addition/Correction*, 2007, **111**, 4726).
41 R. L. Willson, C. L. Greenstock, G. E. Adams, R. Wageman and L. M. Dorfman, *Int. J. Radiat. Phys. Chem.*, 1971, **3**, 211.
42 K. R. Lynn and J. W. Purdie, *Int. J. Radiat. Phys. Chem.*, 1976, **8**, 685.
43 S. Solar, *Radiat. Phys. Chem.*, 1985, **26**, 103.
44 G. V. Buxton, C. L. Greenstock, W. P. Helman and A. B. Ross, *J. Phys. Chem. Ref. Data*, 1988, **17**, 513.
45 V. H. Uc, I. García-Cruz, A. Vivier-Bunge, A theoretical study of the OH radical addition to the xylenes, in *Quantum Systems in Chemistry and Physics*, Advances Problems and Complex Systems, ed. A. Hernandez-Laguna, J. Maruani, R. McWeeny and S. Wilson, Kluwer Academy Publishers, Granada, Spain, 2000, vol II.
46 J. Fan and R. Zhang, *J. Phys. Chem. A*, 2006, **110**, 7728.
47 R. S. Harrison, P. C. Sharpe, Y. Singh and D. P. Fairlie, *Rev. Physiol., Biochem., Pharmacol.*, 2007, **159**, 1.

